Maitotoxin-Induced Calcium Influx in Erythrocyte Ghosts and Rat Glioma C6 Cells, and Blockade by Gangliosides and Other Membrane Lipids

ARTICLE *in* CHEMICAL RESEARCH IN TOXICOLOGY · NOVEMBER 1999

Impact Factor: 3.53 · DOI: 10.1021/tx990014m · Source: PubMed

4 AUTHORS, INCLUDING:

Keiichi Konoki
Tohoku University
49 PUBLICATIONS **1,111** CITATIONS
SEE PROFILE

Michio Murata
Osaka University
224 PUBLICATIONS **7,462** CITATIONS
SEE PROFILE

Maitotoxin-Induced Calcium Influx in Erythrocyte Ghosts and Rat Glioma C6 Cells, and Blockade by Gangliosides and Other Membrane Lipids

Keiichi Konoki, Masaki Hashimoto, Michio Murata,*,† and Kazuo Tachibana

Department of Chemistry, School of Science, The University of Tokyo, Hongo, Bunkyo-ku, Tokyo 113-0033, Japan

Received January 28, 1999

Maitotoxin (MTX) at 0.3 nM elicited a 10−20-fold increase in the level of Ca^{2+} influx in rat glioma C6 cells. At higher doses (3−30 nM), MTX induced marked Ca^{2+} influx in human erythrocyte ghosts when monitored with the fluorescent dye Fura-2. Although the ghosts were not as susceptible to MTX as intact erythrocytes or other cell lines, Fura-2 experiments under various conditions suggested that the MTX-induced entry of ions into the ghosts was mediated by a mechanism similar to that reported for cells or tissues. These ghosts are the simplest system known to be sensitive to MTX and thus may be suitable for research on the direct action of MTX. Gangliosides GM1 and GM3, glycosphingolipids which have a sialic acid residue, strongly inhibited MTX-induced Ca^{2+} influx in C6 cells, while the inhibitory action by asialo-GM1, which lacks a sialic acid residue, was somewhat weaker. Their inhibitory potencies were in the following order: GM1 ($IC_{50} \sim 2\ \mu M$) > GM3 ($IC_{50} \sim 5\ \mu M$) > asialo-GM1 ($IC_{50} \sim 20\ \mu M$). GM1 (3 μM) completely blocked MTX (30 nM)-induced Ca^{2+} influx in human erythrocyte ghosts. When C6 cells were pretreated with tunicamycin, an antibiotic which inhibits N-linked glycosylation, or concanavalin A, a lectin which exhibits a high affinity for cell-surface oligosaccharides, MTX-induced Ca^{2+} influx was significantly potentiated. This suggests that removal of oligosaccharides from the cell surface by tunicamycin or capping of sugar chains on plasma membranes by concanavalin A can potentiate the action of MTX.

Introduction

Maitotoxin (MTX,[1] Figure 1) was first discovered as one of the toxins responsible for ciguatera (*1*), a seafood poisoning caused by ingestion of coral reef fish, and was later shown to be a metabolite of the dinoflagellate *Gambierdiscus toxicus* (*2*). The chemical structure (Figure 1) was recently determined by spectroscopic methods (*3*) and by chemical synthesis (*4*, *5*). The most striking structural feature is the presence of 32 ether rings that are partly substituted with hydroxyl and sulfate groups, which comprise a remarkably large and complicated molecule. Its molecular mass, 3422 Da, is the largest among the known non-biopolymers. In addition to these unique chemical features, MTX has extremely potent bioactivities. Its toxicity is particularly worth noting, since its LD_{50} (50 ng/kg, mouse ip) is exceeded by those of only a few proteinaceous toxins (*3*).

MTX elicits Ca^{2+} influx in virtually all cells and tissues (*6*), and this elevation in intracellular calcium concentration leads to secondary events, e.g., phosphoinositide breakdown (*7*), arachidonic acid release (*8*), muscle contraction (*9*), and secretion of dopamine (*10*), norepinephrine (*11*), and insulin (*12*). MTX-induced Ca^{2+} influx usually occurs concomitantly with depolarization of the membrane potential (*13*). In some excitable cells, MTX-induced Ca^{2+} influx at concentrations below 1 nM has been markedly inhibited by organic and inorganic blockers against voltage-sensitive Ca^{2+} channels (VSCC) (*14*). However, in other cells, the response of MTX is not effectively blocked by VSCC antagonists, but is reduced by other agents, including nonselective cation channel blockers such as SK&F 96365 (*15*). Unlike VSCC, channels activated by MTX have been reported to be rather nonselective, and could pass various cations such as Rb^+, Na^+, Mn^{2+}, and Ba^{2+} (*16*, *17*). These findings suggest that the VSCC are not the primary target of MTX, but are activated by depolarization caused by influx through the primary target.

Recent electrophysiological studies have revealed that channels activated by MTX are nonselective and voltage-independent, since the current−voltage relationship is almost a direct proportion and the reversal potential is nearly zero (*18*). However, other studies indicated that MTX-induced membrane depolarization is essentially independent of Ca^{2+} and due mainly to influx of Na^+ (*17*), which suggests the possibility that the direct action of MTX on biomembranes does not always involve Ca^{2+} influx, but can be due to the entry of other cations. To investigate the primary action of MTX without the influence of secondary cellular events, the use of membrane preparations which lacked intracellular components was preferable. Thus, we became interested in erythrocyte ghosts.

† Present address: Department of Chemistry, Graduate School of Science, Osaka University, 1-16 Machikaneyama, Toyonaka, Osaka 560-0043, Japan. Fax: +81-6-6850-5785. E-mail: murata@ch.wani.osaka-u.ac.jp.

[1] Abbreviations: MTX, maitotoxin; VSCC, voltage-sensitive Ca^{2+} channels; GM1, monosialoganglioside GM1; GM3, monosialoganglioside GM3; Hepes, *N*-(2-hydroxyethyl)piperazine-*N*′-2-ethanesulfonic acid; Fura-2 AM, Fura-2 pentaacetoxymethyl ester; PBS, phosphate-buffered saline.

10.1021/tx990014m CCC: $18.00
Published on Web 09/23/1999

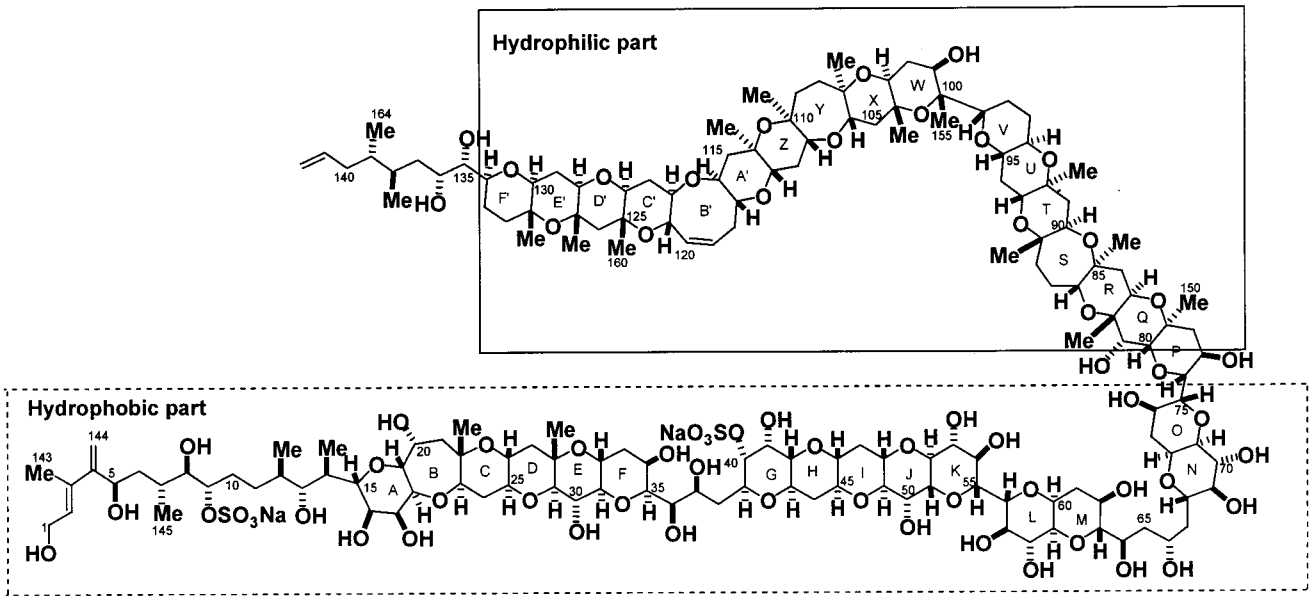

Maitotoxin

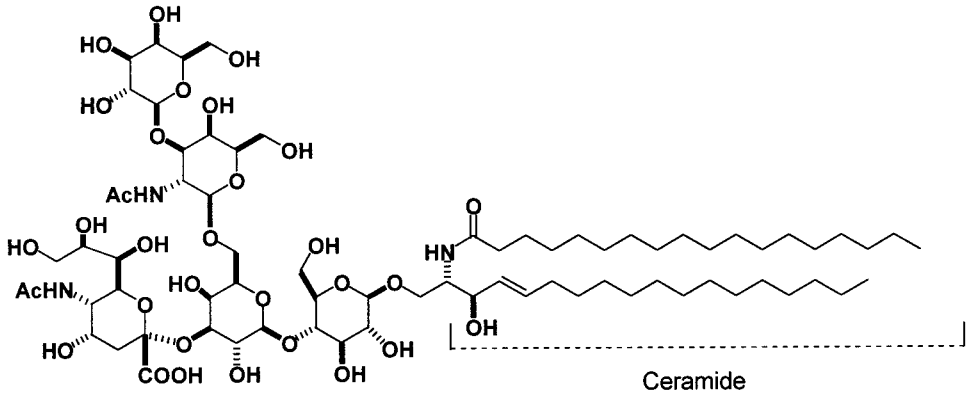

GM1

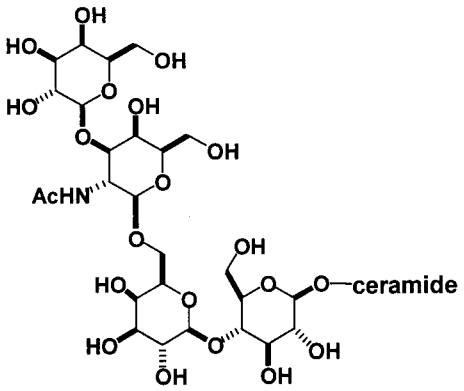

ASGM1

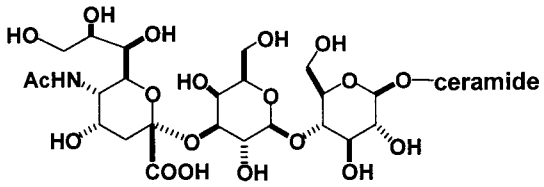

GM3

Figure 1. Absolute structure of maitotoxin (MTX) and those of gangliosides GM1, GM3, and asialo-GM1 (ASGM1).

Many hydrophobic amines have been reported to block the actions of MTX, such as nifedipine, verapamil, SK&F 96365, and tetrahexylammonium salt (*19*, *20*). However, very few non-amine inhibitors have been identified. One example is a glycosphingolipid, ganglioside GM1, which has been reported to be a potent blocker of MTX-induced Ca^{2+} influx in bovine aortic endothelial cells (*21*). The recent establishment of the complete chemical structure of MTX allows us to deduce the three-dimensional shape of the molecule (*4*), which implies a similarity between MTX and glycolipids with regard to their amphiphilicity and possible interactions with biomembranes (Figure 2). The hydrophobic polycyclic ethers from rings R−F′ in MTX (Figure 1) could penetrate into a plasma membrane, as suggested for brevetoxin B (*22*−*25*), whereas the polyhydroxyl groups residing on rings A−Q along with

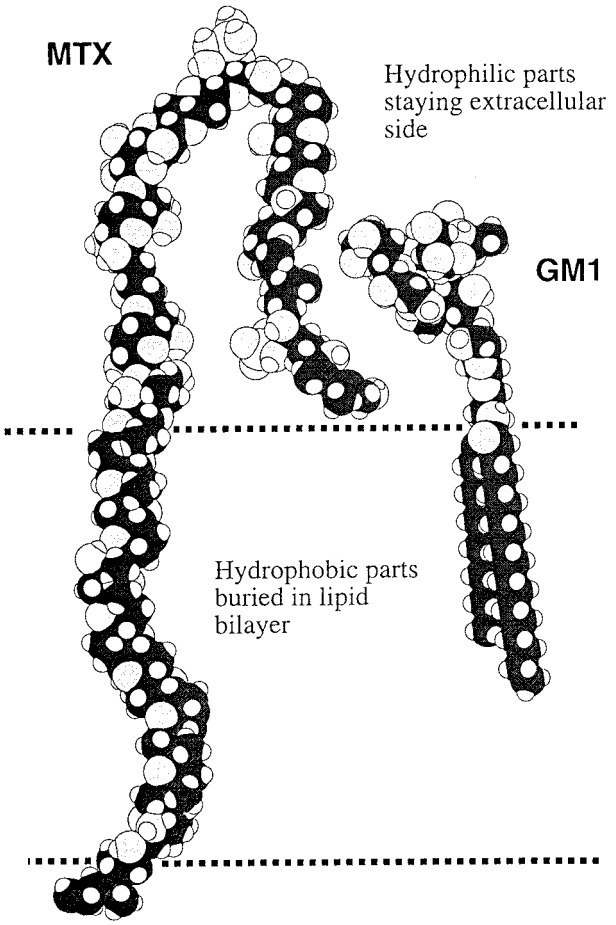

Figure 2. One of the stable conformers for MTX in a space-filling model deduced from NMR data and force-field calculations (*3*, *4*) and that of ganglioside GM1 based on reported data (*40*). Their hydrophobic parts are drawn buried in the lipid bilayer.

two anionic sulfate esters are highly hydrophilic and somewhat mimic the sugar chains of glycolipids. Thus, in this study, we examined the effect of gangliosides tunicamycin and concanavalin A on the MTX-elicited Ca^{2+} influx and depolarization using rat glioma C6 cells and erythrocyte ghosts.

Materials and Methods

MTX was isolated from the French Polynesian strain of the dinoflagellate *G. toxicus* collected off Gambier Island (*2*). The toxin was dissolved in 50% aqueous methanol (290 nM) and kept at −30 °C until it was used. Rat glioma C6 cells, RPMI 1640, a penicillin/streptomycin solution, fetal bovine serum, and trypsin (tissue culture grade) were purchased from Dainippon Pharmaceutical (Osaka, Japan). Gangliosides, ceramide, sulfatide, cardiolipin, and L-α-phosphatidylcholine were purchased from Sigma (St. Louis, MO). Sphingomyelin, Scintisol EX-H, and PC assay kits (Phospholipid B Test-Wako) were from Wako Pure Chemicals (Tokyo, Japan). $^{45}CaCl_2$ and [^{3}H]leucine were from New England Nuclear (Boston, MA). Fura-2 and Fura-2 AM were from Dojindo Laboratory (Kumamoto, Japan). DiS-C_2(5) was a gift from Y. Shai of The Weizmann Institute of Science (Rehovot, Israel).

Cell Culture. Rat glioma C6 cells were cultured at 37 °C in a humidified atmosphere of 5% CO_2/95% air with a CO_2 incubator. The culture medium consisted of RPMI 1640 medium supplemented with 10% fetal bovine serum, 50 units/mL penicillin, and 50 μg/mL streptomycin. C6 cells were grown for 2 days (the cell density usually reached about 2.4×10^6 cells/mL) and inoculated onto new medium to a cell density of 1.2×10^6 cells/mL.

$^{45}Ca^{2+}$ Influx Assays. After passage, rat glioma cells were grown for 2 days, harvested by treatment of trypsin, and diluted to a density of 1.0×10^6 cells/mL. The detached cells were transferred to 12-well plates, and [^{3}H]leucine (0.1 μCi/mL) was added. After overnight incubation, the medium was replaced with 238 μL of buffer A containing 150 mM NaCl, 5 mM KCl, 2 mM $CaCl_2$, 5 mM glucose, and 50 mM Hepes (pH 7.4, adjusted by Tris), along with the agent that was being tested. After preincubation for 13 min, 50 μL of buffer A containing $^{45}CaCl_2$ (1.5 μCi/mL) and 12 μL of MTX solution in 50% aqueous methanol were added to the medium. The cells were incubated for 12 min and then washed three times with buffer A followed by solubilization with 250 μL of 1% sodium dodecyl sulfate (SDS) in 0.5 M NaOH at 37 °C for 20 min. The solution was transferred to a scintillation vial (20 mL), neutralized with 250 μL of 0.5 M HCl, and mixed with 5 mL of Scintisol EX-H. The radioactivity was measured with a scintillation counter (Tricarb 2200CA, Hewlett-Packard) set for simultaneous counting of ^{3}H and ^{45}Ca. Differences in the growth of the cells among microplate wells were normalized by the ^{3}H count for incorporated [^{3}H]leucine.

Preparation of Fura-2-Loaded C6 Cells and Intact Erythrocytes. To monitor the intracellular Ca^{2+} concentration, the fluorescent dye Fura-2 AM was loaded into the C6 cells. Glioma C6 cells cultured for 2 days after splitting were used for the assays. The cells were loaded with Fura-2 by incubation for 40 min at 32 °C with 3 μM Fura-2 AM in the culture medium. The cells were washed twice with buffer A without glucose and resuspended in the same buffer at a cell density of 3×10^5 cells/mL for fluorescence measurements. Human erythrocytes were washed and loaded with Fura-2 using Fura-2 AM in the same manner described for C6 cells. For the fluorescence measurement, the erythrocytes were suspended in the same buffer at a density of 1.1×10^8 cells/mL, a density at which the concentration of phosphatidylcholine (PC) was 36 μg/mL; the amount of lipid was determined by a PC assay kit. $CaCl_2$ (2 mM) was added prior to fluorescent measurements.

Preparation of Fura-2-Loaded Erythrocyte Ghosts. Erythrocyte ghosts were prepared basically according to the method of Kracke (*26*). Fresh human blood (5−10 mL) was heparinized and washed four times by centrifugation (2000*g* for 15 min) in PBS(−) at 4 °C. Packed erythrocytes were lysed on ice for 10 min in 100 mL of a hypotonic lysing buffer containing 7 mM KCl and 5 mM Tris (pH 7.4). The membranes were centrifuged at 30000*g* for 15 min and washed four times in 10 mL of the same lysing buffer. Before the ghosts were resealed, the osmolarity was adjusted by adding a buffer containing 1.5 M KCl, 10 mM $MgCl_2$, and 10 mM dithiothreitol (until the final KCl concentration was 150 mM) in the presence of 1 mM Fura-2. Ghosts were resealed by incubating at 37 °C for 30 min. The resultant ghosts were centrifuged at 25000*g* at 4 °C for 15 min and washed with 10 mL of buffer A without glucose. The ghosts were washed four more times to remove unincorporated Fura-2. For the assay of Ca^{2+} influx, ice-cold ghosts were resuspended in 1 mL of the same buffer at 37 °C in cuvettes at a density at which the PC content was 36 μg/mL. $CaCl_2$ (2 mM) was added prior to fluorescent measurements.

Fluorescent Measurements for Monitoring the Intracellular Ca^{2+} Concentration. Intracellular Ca^{2+} concentrations were monitored using the fluorescence ratio upon dual excitation at 340 and 380 nm, as described by Grynkiewicz et al. (*27*). Fluorescence was measured in a 3 mL cuvette containing 1 mL of the suspension with a spectrofluorophotometer (RF-1500, Shimadzu) while the cuvette was maintained at 37 °C and its contents were stirred by a magnetic stirrer. The dual excitation wavelength was set at 340 and 380 nm, and the emission wavelength was 510 nm. In Figures 4, 5, and 7, the ratio ($R = F_{340}/F_{380}$) of fluorescence intensities upon excitation at 340 and 380 nm was taken to be the ordinate, which corresponded to the intracellular Ca^{2+} concentrations (*28*). The concentration of intracellular Ca^{2+} was calculated for the traces

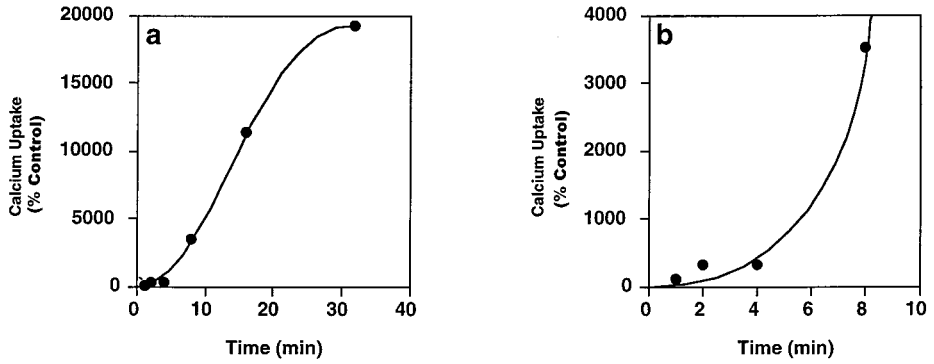

Figure 3. (a) Typical time course of MTX-induced $^{45}Ca^{2+}$ influx in rat glioma C6 cells. C6 cells (1×10^6 cells) were cultured in 12-well plates in the presence of [^{3}H]leucine (0.1 μCi/mL) at 37 °C for 19 h. After preincubation in a buffer consisting of 150 mM NaCl, 5 mM KCl, 2 mM $CaCl_2$, 5 mM glucose, and 50 mM Hepes/Tris (pH 7.4) for 13 min, the cells were incubated for each indicated period of time (1, 2, 4, 8, 16, and 32 min) with $^{45}Ca^{2+}$ (1.5 μCi/mL) and MTX in the same buffer. The cells were then washed, and the $^{45}Ca^{2+}$ content was determined as described in Materials and Methods. Values are the means from a single experiment performed in duplicate. The other two experiments showed a similar tendency where the level of influx increased rapidly after 5−10 min and became saturated at about 30 min, although poor reproducibility in the magnitude of the influx among the experiments prevented statistical treatments. The percentage of control calcium influx equals the amount of calcium influx relative to the amount at 1 min. (b) Same trace as that in panel a except for an expanded scale for the period of 0−10 min.

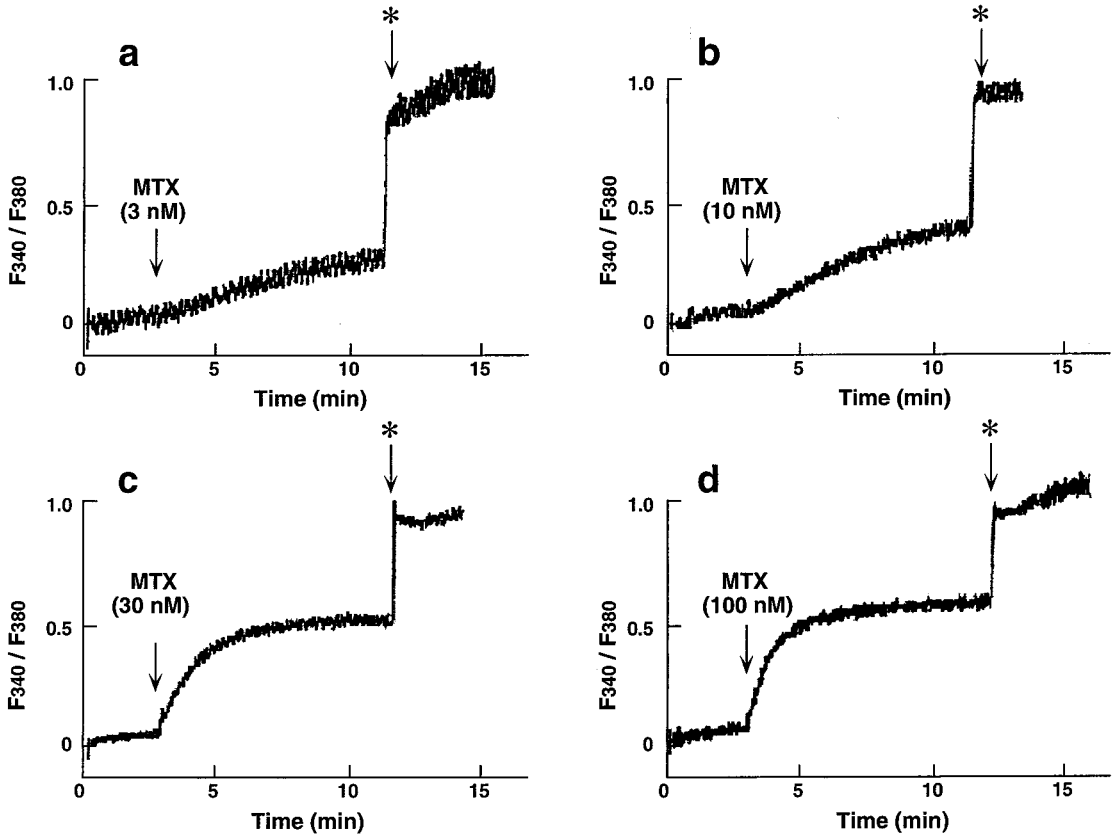

Figure 4. Dose−effect relationship of MTX-induced Ca^{2+} influx in human erythrocyte ghosts. Erythrocyte ghosts entrapped with Fura-2 were prepared as described in Materials and Methods. Several minutes after addition of 2 mM $CaCl_2$, MTX at (a) 3, (b) 10, (c) 30, or (d) 100 nM was added to Fura-2-containing ghosts. After the fluorescence trace became saturated, Triton X-100 (0.2%) was added at the points indicated by asterisks to solubilize the ghosts. The experiment was repeated three times with similar results.

in Figure 4a−d according to a published method (*27*) to determine the initial rates of Ca^{2+} influx. The total concentration of Fura-2 trapped in cells was estimated by self-quenching of fluorescence. The *R* value after saturation with a high concentration of MTX or A23187 was taken to be the maximal ratio, and that obtained by subsequent addition of 20 mM EGTA was taken to be the minimal ratio.

Fluorescent Dye [DiS-C_2(5)] Experiments for Measuring the Membrane Potential of C6 Cells. C6 cells were prepared by the same procedure that was used for the Fura-2 experiments, except that DiS-C_2(5) (*29*) was used instead of Fura-2 AM. One-milliliter aliquots of the cell suspension were added to a final DiS-C_2(5) concentration of 1 μM in 5 μL of MeOH 10 min before the fluorescence measurement. Fluorescence was measured in the same manner as in the Fura-2 experiments except excitation and emission wavelengths were 620 and 675 nm, respectively.

Results

MTX-Induced Ca^{2+} Influx in C6 Cells and in Erythrocyte Ghosts. We used two different methods to measure the level of Ca^{2+} influx into cells and erythrocyte ghosts; one employs radioactive $^{45}Ca^{2+}$ influx,

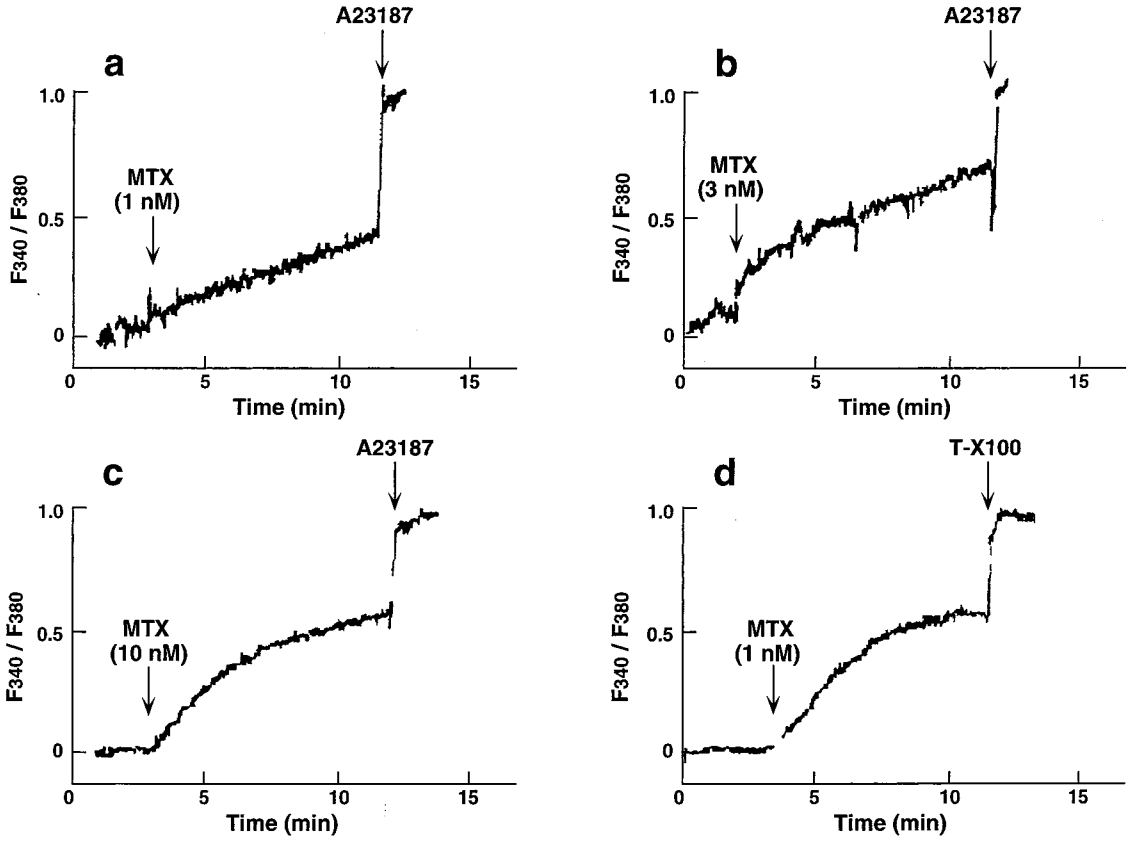

Figure 5. MTX-induced Ca^{2+} influx in intact human erythrocytes at various doses (a−c) and in rat glioma C6 cells (d). (a−c) Fura-2-entrapped human erythrocytes were prepared with Fura-2 AM as described in Materials and Methods. The Fura-2-loaded erythrocytes were incubated with MTX at (a) 1, (b) 3, or (c) 10 nM in the presence of 2 mM $CaCl_2$. After the Ca^{2+} influx reached a plateau, the Ca^{2+} ionophore A23187 was added to the suspension. The experiment was repeated three or more times with similar results. (d) C6 cells were loaded with Fura-2 by incubation with Fura-2 AM (3 μM) for 40 min at 32 °C. After being washed twice, the cells were suspended at a density of 3×10^5 cells/mL in buffer and subjected to fluorescence measurements as described in Materials and Methods. The experiment was repeated three or more times with similar results.

and the other employs a fluorescent dye, Fura-2. The radioisotope experiment was used for the quantitative evaluation of Ca^{2+} influx because of its better experimental reproducibility and wider range of measurable Ca^{2+} concentrations. Thus, we adopted this method for the inhibitory (Figures 6 and 9) and potentiation effects (Figure 8) of drugs. The Fura-2 method, even with its narrow dynamic range and the difficulty in statistical treatments, provides a great advantage in monitoring time-dependent changes (Figures 4, 5, and 7). For the time course of Ca^{2+} influx in C6 cells (Figure 3), however, we used the $^{45}Ca^{2+}$ assay since the Ca^{2+} concentrations at the later stages were too high to measure by the Fura-2 method.

As reported previously by Sladeczek et al. (*30*), MTX stimulated $^{45}Ca^{2+}$ influx in rat glioma C6 cells in a dose-dependent manner. The time course of the influx of $^{45}Ca^{2+}$ in C6 cells (Figure 3) appeared to be different from that of the Fura-2-monitored intracellular Ca^{2+} influx (Figure 5d). This can be explained by the difference in the ranges of Ca^{2+} concentrations that can be measured by $^{45}Ca^{2+}$ influx assays and by Fura-2 experiments; the former is suited for Ca^{2+} concentrations ranging from 10 μM to 1 mM, while the latter is usually used for Ca^{2+} levels from 0.1 μM to the Fura-2 concentration, which in these assays was estimated to be ca. 20 μM on the basis of the cell size and the concentration of Fura-2 after lysing the cells (*31*). In the $^{45}Ca^{2+}$ assays (Figure 3), the initial influx as seen in the Fura-2 experiments was thought to occur,

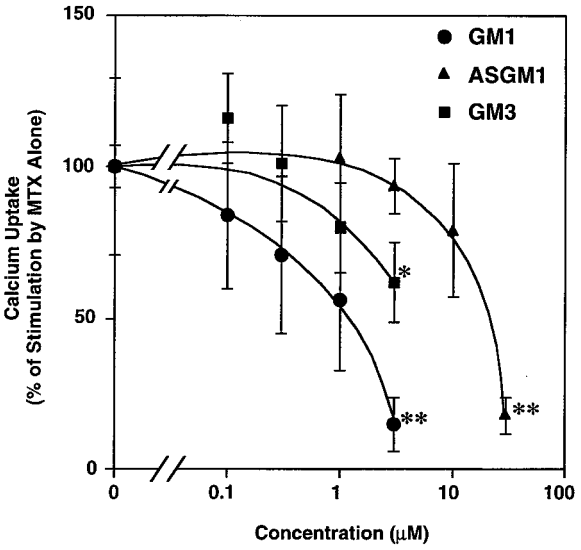

Figure 6. Blockade of MTX-induced $^{45}Ca^{2+}$ influx in rat glioma C6 cells by gangliosides. C6 cells (1×10^6 cells) were preincubated with ganglioside GM1 (●), asialoganglioside GM1 (▲), or ganglioside GM3 (■) for 13 min. The incubation for $^{45}Ca^{2+}$ influx was started by the addition of MTX (0.6 nM) and $^{45}Ca^{2+}$ (1.5 μCi/mL) to the cells. After 12 min, the cells were washed and the $^{45}Ca^{2+}$ content was determined as described in Materials and Methods. Values correspond to means ± standard errors of three independent experiments, each performed in duplicate. The significance of the effects was determined by a Student's *t* test (one asterisk, $P < 0.05$; two asterisks, $P < 0.01$) compared to the control.

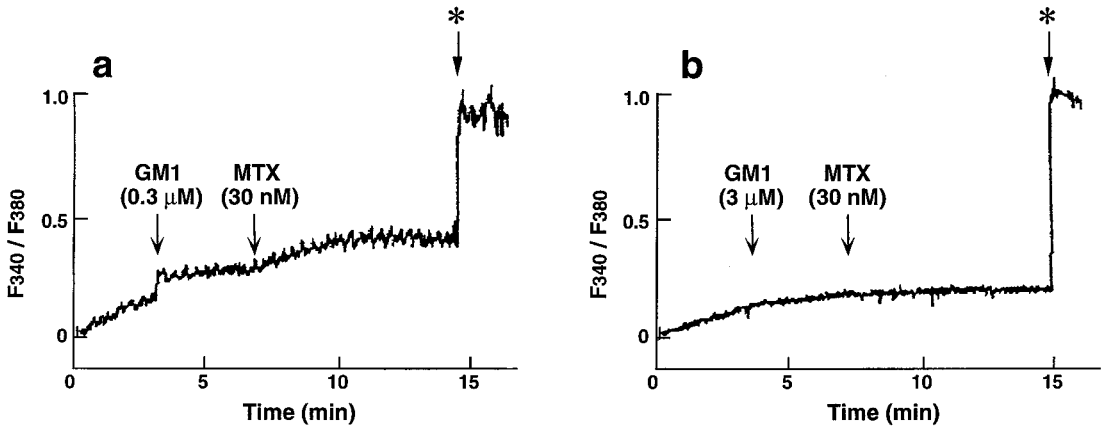

Figure 7. Blockade of MTX-induced Ca^{2+} influx in human erythrocyte ghosts by ganglioside GM1. Fura-2-loaded erythrocyte ghosts were prepared as described in Materials and Methods. The ghosts were subjected to fluorescence measurements. Each concentration of GM1 [(a) 0.3 and (b) 3 μM] and 30 nM MTX were added to the cells. After the fluorescence intensity became constant, Triton X-100 (0.2%) was added at the points indicated by asterisks to solubilize the ghosts. The experiment was repeated three times with similar results.

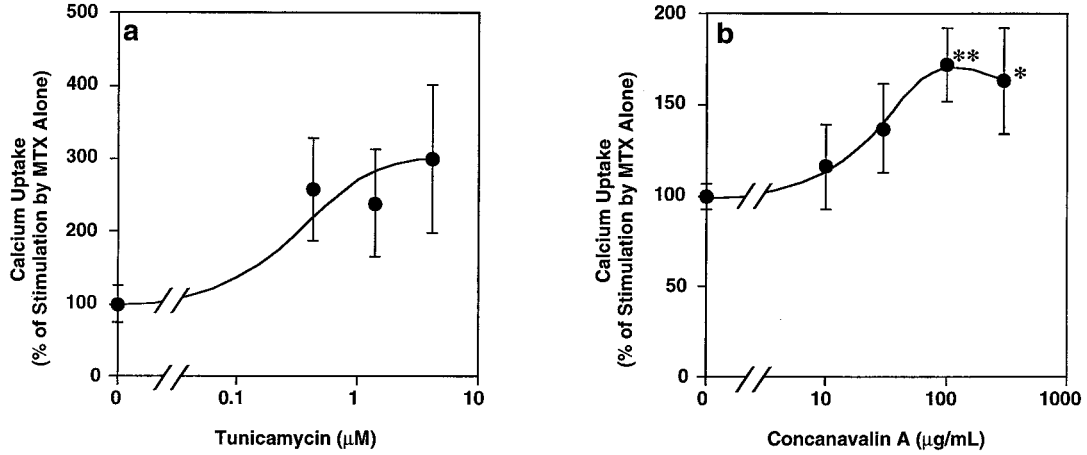

Figure 8. Potentiation of MTX-induced $^{45}Ca^{2+}$ influx in rat glioma C6 cells by tunicamycin (a) or concanavalin A (b). (a) After preincubation for 19 h in the presence of tunicamycin or (b) after preincubation for 13 min in the presence of concanavalin A, the cells (1×10^6 cells) were incubated for 12 min in the presence of MTX (1 nM) and $^{45}Ca^{2+}$ (1.5 μCi/mL). Intracellular Ca^{2+} concentrations were determined as described in Materials and Methods. Values correspond to means ± standard errors of three independent experiments, each performed in duplicate. The significance of the effects was determined by a Student's *t* test (one asterisk, $P < 0.05$; two asterisks, $P < 0.01$) compared to the control.

although the magnitude of the influx was too small to be detected.

Fura-2 experiments revealed that MTX (3−100 nM) induced Ca^{2+} influx in erythrocyte ghosts, as shown in Figure 4. Since the concentration of Fura-2 in the ghosts was estimated to be 20 μM, the fluorescence intensity became saturated above 10 μM Ca^{2+} and deviated from a proportional relation to the Ca^{2+} concentration, particularly near saturation levels. Therefore, increases in the intracellular Ca^{2+} concentration elicited by MTX should be expressed as the initial rate obtained from a tangent of each trace at a point immediately after the addition of MTX; from the traces in Figure 4a−d, the initial rates at 3, 10, 30, and 100 nM MTX were estimated to be 3.1, 4.3, 6.7, and 11.6 μM/min, respectively. The MTX-induced Ca^{2+} increase in erythrocyte ghosts started immediately after the addition of MTX. The time course was comparable to those for intact erythrocytes (Figure 5a−c) and C6 cells (Figure 5d), although the concentration of MTX needed to induce an increase in the Ca^{2+} concentration in ghosts was higher than those needed for whole erythrocytes or C6 cells. Intracellular Fura-2 did not significantly leak from erythrocyte ghosts or C6 cells because of addition of MTX at the concentrations that were tested. Fluorescence intensity in the absence of extracellular Ca^{2+} was unchanged, which suggested that Fura-2 did not go out of the cells or ghosts; if it happened, the intensity should have increased due to recovery from self-quenching of entrapped Fura-2.

Inhibition of MTX-Induced $^{45}Ca^{2+}$ Influx by Gangliosides GM1, Asialo-GM1, and GM3. The ganglioside GM1 inhibited MTX (0.6 nM)-induced $^{45}Ca^{2+}$ influx in C6 cells in a dose-dependent manner with an IC_{50} of 2 μM (Figure 6). Ganglioside GM3, which has fewer sugars than GM1, and asialo-GM1, which lacks a sialic acid residue, were somewhat weaker inhibitors than GM1 (Figure 6); the IC_{50} values of these gangliosides were in the following order: GM1 (2 μM) > GM3 (5 μM) > asialo-GM1 (20 μM). Treatment of C6 cells with GM1 in a preincubation period, followed by depleting GM1 during incubation, still caused inhibition of MTX-induced $^{45}Ca^{2+}$ influx in C6 cells; pretreatment with 1 μM GM1 and 10 μM GM1 reduced the level of influx to 70 and 12% of that with MTX alone, respectively. MTX-induced Ca^{2+} influx in erythrocyte ghosts was also inhibited by ganglioside GM1 (Figure 7). The potency of the inhibition by GM1 was comparable to that in C6 cells.

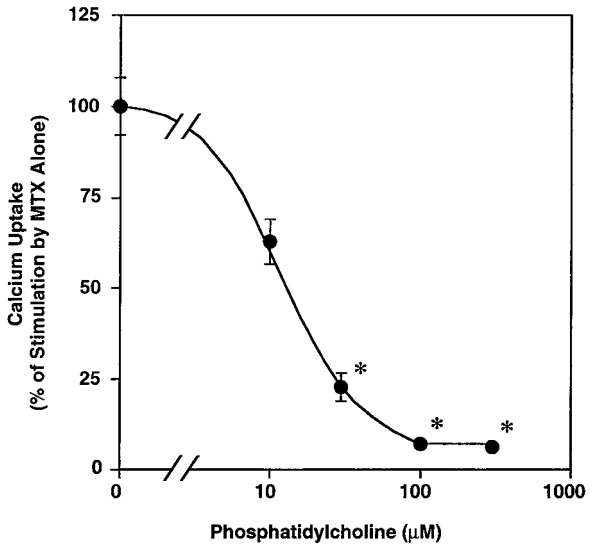

Figure 9. Blockade of MTX-induced $^{45}Ca^{2+}$ influx in rat glioma C6 cells by phosphatidylcholine (PC). Cells (1×10^6 cells) were preincubated for 13 min in the presence of phosphatidylcholine as small unilamellar vesicles (SUV), and after the addition of MTX (1.0 nM) and $^{45}Ca^{2+}$ (1.5 μCi/mL), the cells were incubated for an additional 12 min. The cells were washed, and the $^{45}Ca^{2+}$ content was determined as described in Materials and Methods. Values correspond to means ± standard errors of three independent experiments, each perfomed in duplicate. The significance of the effects was determined by a Student's *t* test (one asterisk, $P < 0.01$) compared to the control.

Potentiation of MTX-Induced $^{45}Ca^{2+}$ Influx by Tunicamycin and Concanavalin A. Since glycolipids inhibited the actions of MTX, we next attempted to modify the glycoside residues on the cell surface using tunicamycin (*32*) and concanavalin A (*33*). Tunicamycin is known to inhibit both glycosylation for proteins and synthesis of lipid-linked oligosaccharides. After exposure of C6 cells to tunicamycin (0.3−10 μM) for 19 h prior to the assays, MTX (1 nM)-induced $^{45}Ca^{2+}$ influx was potentiated in a dose-dependent manner; pretreatment with tunicamycin (0.42 μM) induced a ~2.5-fold increase in the level of $^{45}Ca^{2+}$ influx compared with that with MTX alone (Figure 8a). In the presence of concanavalin A (100 μg/mL), a lectin which binds to oligosaccharide chains on the cell surface, MTX (1 nM)-induced $^{45}Ca^{2+}$ influx was enhanced by 1.7-fold (Figure 8b). These results suggest that MTX has an affinity for oligosaccharides on the cell surface, and their removal by tunicamycin or blockade by concanavalin A reduces the level of nonspecific binding of MTX to sugar chains, which should result in an increase in the concentration of MTX that is accessible to target molecule(s).

Inhibition of MTX-Induced $^{45}Ca^{2+}$ Influx by Membrane Lipids. Since glycolipids such as gangliosides inhibited the actions of MTX, we next examined the effects of a ubiquitous membrane constituent. Phosphatidylcholine (PC), a common membrane lipid, blocked MTX-induced $^{45}Ca^{2+}$ influx in C6 cells; the IC_{50} values of PC in the form of small unilamellar vesicles (SUV) was 20 μM (Figure 9). Pretreatment of C6 cells with PC (micelles) before the addition of MTX also significantly inhibited the action of MTX ($IC_{50} \sim 30$ μM, data not shown). These results strongly suggest that MTX is absorbed by the added PC micelles or vesicles, which reduces the effective concentration of MTX.

To evaluate the role of a polar headgroup in membrane lipids, we tested several membrane constituents for their inhibitory actions against MTX-induced $^{45}Ca^{2+}$ influx in C6 cells, e.g., ceramide, sulfatide, cardiolipin, and sphingomyelin. Among these, sphingomyelin, sphingolipid bearing a phosphocholine residue, produced prominent blockade with an IC_{50} of ca. 10 μM. However, ceramide and cardiolipin showed no significant inhibition at 100 μM.

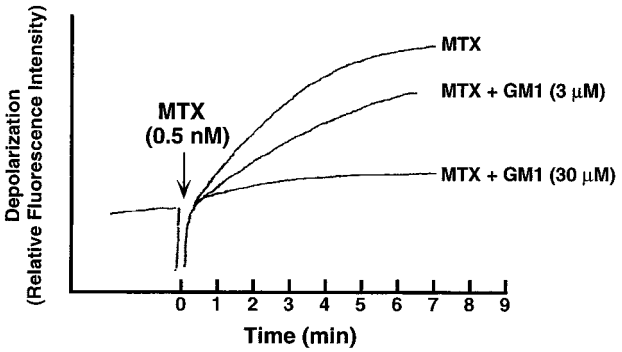

Figure 10. Blockade of MTX-induced membrane depolarization by ganglioside GM1. C6 cells (3×10^5 cells/mL) were loaded with 1 μM DiS-C_2(5) as described in Materials and Methods. After a steady baseline value was obtained, the cell suspensions were either left untreated or treated with 3 or 30 μM ganglioside GM1. After the fluorescence trace became steady, the cells were treated with 0.5 nM MTX in the presence of 2 mM $CaCl_2$. The experiment was repeated three times with similar results.

Discussion

The biological actions of MTX have been investigated for two decades in tissues, cells, synaptosomes, and vesicles. MTX elicited Ca^{2+} influx in all tissues and cells (*6*). MTX does not elicit Ca^{2+} entry into artificial phospholipid vesicles (*16*, *34*) but does induce Ca^{2+} influx in synaptosomes (*35*, *36*), which are derived from brain neuronal membranes and usually contain diluted cytoplasmic constituents. The study presented here has demonstrated that MTX stimulates Ca^{2+} influx in erythrocyte ghosts, which are completely vacant vesicles, and hence are the simplest material that is known to be sensitive to MTX. The prominent difference between ghosts and artificial vesicles is the respective presence and absence of diverse membrane components such as proteins or glycolipids, which most likely include the primary target of MTX. Therefore, erythrocyte ghosts provide an excellent model system for investigation of the direct site of action of MTX.

Bressler et al. (*21*) reported that ganglioside GM1 blocked MTX-induced Ca^{2+} influx in bovine aortic endothelial cells. The study presented here has demonstrated that GM1 binding to plasma membranes of C6 cells and erythrocyte ghosts antagonizes the MTX response, and that GM3 and asialo-GM1, although weaker than GM1, also antagonize the MTX-induced Ca^{2+} influx in C6 cells. We also observed that GM1 blocked the MTX-induced depolarization of C6 cells (Figure 10). In our previous study (*20*), alkylamines such as trihexylamine and tetrahexylammonium salt blocked MTX-induced Ca^{2+} uptake, but did not inhibit depolarization. Dietl and Völkl (*37*) reported that Ca^{2+} entry probably lies relatively downstream in the cascade of MTX-induced events on the basis of their observation that a nonselective ion current precedes Ca^{2+} influx. The study presented here supports these findings by implying that MTX-induced Ca^{2+} influx is mediated by ion channels which can be blocked by

alkylamines, whereas MTX-elicited depolarization, which is probably caused by different channels, can be inhibited by gangliosides but not by alkylamines (*20*).

To investigate the role of glycoside residues on lipids as well as those on membrane proteins, we treated C6 cells with tunicamycin and concanavalin A. Both treatments potentiated MTX-induced Ca^{2+} influx, while each agent alone induced no influx. Our interpretation of the results is as follows. Sugar residues which would have affinity for MTX are reduced by these agents, and thus, more MTX becomes available to the primary target for the actions of MTX. Gangliosides and other glycolipids are found only in the outer monolayer of plasma membranes. The oligosaccharide residues protrude from the outer layer, and the hydrocarbon chains anchor the molecule to plasma membranes. We have previously investigated the conformation of MTX by means of NMR and force field calculations (*3*, *4*); the hydrophobic portion of MTX appeared to be mainly extended, while the hydrophilic part had a flexible structure with a major conformer in which it is bent like a hairpin as shown in Figure 2 (*4*). Therefore, the gross stereostructure of MTX resembles that of gangliosides, particularly with regard to the hydrophilic portion. Gangliosides are known to undergo self-aggregation to form stable clusters on biomembranes (*38*, *39*). After MTX is incorporated into such a cluster, a high affinity for gangliosides should retain an MTX molecule within the cluster. This could explain the potent and nonselective blockade of the actions of MTX by gangliosides.

To gain a better understanding of the mechanism of MTX-induced actions, identification of the primary target is required, perhaps through labeling the receptor molecule with MTX or chemically modified analogues.

Acknowledgment. We are grateful to Prof. Takeshi Yasumoto (Tohoku University, Tohoku, Japan) for generously providing us with maitotoxin and for discussions throughout this study. We also thank Dr. J. W. Daly of the National Institute of Diabetes and Digestive and Kidney Diseases (National Institutes of Health, Bethesda, MD) for helpful comments and suggestions. We also thank Mr. N. Nogawa and Dr. K. Tao of the Radioisotope Center of The University of Tokyo for their assistance and Dr. M. Sasaki and Dr. T. Nonomura in our laboratory for discussion on the three-demensional structure of MTX. This study was supported in part by a grant-in-aid (Priority Area Research of "Natural Supramolecules") from the Ministry of Education, Science, and Culture, Japan, by the Research for the Future Program of the Japan Society for the Promotion of Science (JSPS-RFTF96I00301), and by the Nissan Science Foundation.

References

(1) Yasumoto, T., Bagnis, R., and Vernoux, J. P. (1976) Toxicity of surgeonfish 2. Properties of the principal water-soluble toxin. *Bull. Jpn. Soc. Fish.* **42**, 359−365.

(2) Yokoyama, A., Murata, M., Oshima, Y., Iwashita, T., and Yasumoto, T. (1988) Some chemical properties of maitotoxin, a putative calcium channel agonist isolated from a marine dinoflagellate. *J. Biochem.* **104**, 184−187.

(3) Murata, M., Naoki, H., Matsunaga, S., Satake, M., and Yasumoto, T. (1994) Structure and partial stereochemical assignments for maitotoxin, the most toxic and largest natural non-biopolymer. *J. Am. Chem. Soc.* **116**, 7098−7107.

(4) Sasaki, M., Matsumori, N., Maruyama, T., Nonomura, T., Murata, M., Tachibana, K., and Yasumoto, T. (1996) The complete structure of maitotoxin, part I: Configuration of the C1−C14 side chain. *Angew. Chem., Int. Ed.* **35**, 1672−1675.

(5) Zheng, W., DeMattei, J. A., Wu, J.-P., Duan, J. J.-W., Cook, L. R., Oinuma, H., and Kishi, Y. (1996) Complete relative stereochemistry of maitotoxin. *J. Am. Chem. Soc.* **118**, 7946−7968.

(6) Gusovsky, F., and Daly, J. W. (1990) Maitotoxin: a unique pharmacological tool for research on calcium-dependent mechanisms. *Biochem. Pharmacol.* **39**, 1633−1639.

(7) Gusovsky, F., Yasumoto, T., and Daly, J. W. (1989) Maitotoxin, a potent, general activator of phosphoinositide breakdown. *FEBS Lett.* **243**, 307−312.

(8) Choi, O. H., Padgett, W. L., Nishizawa, Y., Gusovsky, F., Yasumoto, T., and Daly, J. W. (1989) Maitotoxin: effects on calcium channels, phosphoinositide breakdown, and arachinodate release in pheochromocytoma PC12 cells. *Mol. Pharmacol.* **37**, 222−230.

(9) Ohizumi, Y., Kajiwara, A., and Yasumoto, T. (1983) Excitatory effect of the most potent marine toxin, maitotoxin, on the Guinea-pig vas deferens. *J. Pharmacol. Exp. Ther.* **227**, 199−204.

(10) Taglialatela, M., Amoroso, S., Yasumoto, T., Renzo, G. D., and Annunziato, L. (1986) Maitotoxin and BAY-K-8644: two putative calcium channel activators with different efects on endogeneous dopamine release from tuberoinfundibular neurons. *Brain Res.* **381**, 356−358.

(11) Takahashi, M., Tatsumi, M., Ohizumi, Y., and Yasumoto, T. (1983) Ca^{2+} channel activating function of maitotoxin, the most potent marine toxin known, in clonal rat pheochromocytoma cells. *J. Biol. Chem.* **258**, 10944−10949.

(12) Soergel, D., Gusovsky, F., Yasumoto, T., and Daly, J. W. (1990) Stimulatory effects of maitotoxin on insulin release in insulinoma HIT cells: role of calcium uptake and phosphoinositide breakdown. *J. Pharmacol. Exp. Ther.* **255**, 1360−1365.

(13) Xi, D., Dolah, F. M. V., and Ramsdell, J. S. (1992) Maitotoxin induces a calcium-dependent membrane depolarization in GH_4C_1 pituitary cells via activation of type L voltage-dependent calcium channels. *J. Biol. Chem.* **267**, 25025−25031.

(14) Xi, D., Kurtz, D. T., and Ramsdell, J. S. (1996) Maitotoxin-elevated cytosolic free calcium in GH_4C_1 rat pituitary cells nimodipine-sensitive and -insensitive mechanisms. *Biochem. Pharmacol.* **51**, 759−769.

(15) Soergel, D., Yasumoto, T., Daly, J. W., and Gusovsky, F. (1992) Maitotoxin effects are blocked by SK&F 96365, an inhibitor of receptor-mediated calcium entry. *Mol. Pharmacol.* **41**, 487−493.

(16) Murata, M., Gusovsky, F., Yasumoto, T., and Daly, J. W. (1992) Selective stimulation of Ca^{2+} flux in cells by maitotoxin. *Eur. J. Pharmacol.* **227**, 43−49.

(17) Nishio, M., Muramatsu, I., and Yasumoto, T. (1996) Na-permeable channels induced by maitotoxin in Guinea-pig single ventricular cells. *Eur. J. Pharmacol.* **297**, 293−298.

(18) Escobar, L. I., Salvador, C., Martinez, M., and Vaca, L. (1998) Maitotoxin, a cationic channel activator. *Neurobiology* **6**, 59−74.

(19) Daly, J. W., Lueder, J., Padgett, W. L., Yangmee, S., and Gusovsky, F. (1995) Maitotoxin-elicited calcium influx in cultured cells: effect of calcium-channel blockers. *Biochem. Parmacol.* **50**, 1187−1197.

(20) Konoki, K., Hashimoto, M., Murata, M., Tachibana, K., and Yasumoto, T. (1996) Blockade of MTX-induced Ca^{2+} influx in rat glioma C6 cells by alkylamines. *J. Nat. Toxins* **5**, 209−217.

(21) Bressler, J. P., Belloni-Olivi, L., and Forman, S. (1993) Effect of ganglioside GM1 on arachidonic acid release in bovine aortic endothelial cells. *Life Sci.* **54**, 49−60.

(22) Trainer, V. L., Baden, D. G., and Catterall, W. A. (1994) Identification of peptide components of the brevetoxin receptor site of rat brain sodium channels. *J. Biol. Chem.* **269**, 19904−19909.

(23) Gawley, R. E., Rein, K. S., Jeglitsch, G., Adams, D. J., Theodorakis, E. A., Tiebes, J., Nicolaou, K. C., and Baden, D. G. (1995) The relationship of brevetoxin "length" and A-ring functionality to binding and activity in neuronal sodium channels. *Chem. Biol.* **2**, 533−541.

(24) Matile, S., Berova, N., and Nakanishi, K. (1996) Exciton coupled circular dichroic studies of self-assembled brevetoxin-porphyrin conjugates in lipid bilayers and polar solvents. *Chem. Biol.* **3**, 379−392.

(25) Matile, S., and Nakanishi, K. (1996) Selective cation movement across lipid bilayers containing brevetoxin B. *Angew. Chem., Int. Ed.* **35**, 757−759.

(26) James-Kracke, M. R. (1992) Calmodulin activation of the Ca^{2+} pump revealed by fluorescent chelator dyes in human red blood cell ghosts. *J. Gen. Physiol.* **99**, 41−62.

(27) Grynkiewicz, G., Poenie, M., and Tsien, R. Y. (1985) A new generation of Ca^{2+} indicators with greatly improved fluorescence properties. *J. Biol. Chem.* **260**, 3440−3450.

(28) Roe, M. W., Worley, J. F., III, Qian, F., Tamarina, N., Mittal, A. A., Dralyuk, F., Blair, N. T., Mertz, R. J., Philipson, L. H., and Dukes, I. D. (1998) Characterization of a Ca^{2+} release-activated nonselective cation current regulating membrane potential and $[Ca^{2+}]_i$ oscillations in transgenically derived β-cells. *J. Biol. Chem.* **263**, 10402−10410.

(29) Loew, L. M., Benson, L., Lazarovici, P., and Rosenberg, I. (1985) Fluorometric analysis of transferable membrane pores. *Biochemistry* **24**, 2101−2104.

(30) Sladeczek, F., Schmidt, B. H., Alonso, R., Vian, L., Tep, A., Yasumoto, T., Cory, R. N., and Bockaert, J. (1988) New insights into maitotoxin action. *Eur. J. Biochem.* **174**, 663−670.

(31) Thomas, A. P., and Delaville, F. (1991) The use of fluorescent indicators for measurements of cytosolic-free calcium concentration in cell populations and single cells. In *Cellular Calcium* (McCormack J. G., and Cobbold, P. H., Eds.) pp 1−53, IRL Press, Oxford, U.K.

(32) Leavitt, R., Schlesinger, S., and Kornfeld, S. (1977) Tunicamycin inhibits glycosylation and multiplication of sindbis and vesicular stomatitis viruses. *J. Virol.* **21**, 375−385.

(33) Burger, M. M., and Noonan, K. D. (1970) Restoration of normal growth by covering of agglutinin sites on tumor cell surface. *Nature* **228**, 512−515.

(34) Takahashi, M., Ohizumi, Y., and Yasumoto, T. (1982) Maittotoxin, a Ca^{2+} channel activator candidate. *J. Biol. Chem.* **257**, 7287−7289.

(35) Ueda, H., Tamura, S., Fukushima, N., and Takagi, H. (1986) Pertussis toxin (IAP) enhances maitotoxin (a putative Ca^{2+} channel agonist)-induced Ca^{2+} entry into synaptosomes. *Eur. J. Pharmacol.* **122**, 379−380.

(36) Taglialatela, M., Canzoniero, L. M. T., Fatatis, A., Renzo, G. D., Yasumoto, T., and Annunziato, L. (1990) Effect of maitotoxin on cytosolic Ca^{2+} levels and membrane potential in purified rat brain synaptosomes. *Biochim. Biophys. Acta* **1026**, 126−132.

(37) Dietl, P., and Völkl, H. (1993) Maitotoxin activates a nonselective cation channel and stimulates Ca^{2+} entry in MDCK renal epithelial cells. *Mol. Pharmacol.* **45**, 300−305.

(38) Thompson, T. E., and Tillack, T. W. (1985) Organization of glycosphingolipids in bilayers and plasma membranes of mamalian cells. *Annu. Rev. Biophys. Biophys. Chem.* **14**, 361−386.

(39) Miller-Podraza, H., Bradley, R. M., and Fishman, P. H. (1982) Biosynthesis and localization of gangliosides in cultured cells. *Biochemistry* **21**, 3260−3265.

(40) Acquotti, D., Fronza, G., Ragg, E., and Sonnino, S. (1991) Three-dimensional structure of GD1b and GD1b-monolactone gangliosides in dimethylsulphoxide: a nuclear Overhauser effect investigation supported by molecular dynamics calculations. *Chem. Phys. Lipids* **59**, 107−125.

TX990014M